Experimental and Numerical Study on Cavitation Effects
in Centrifugal Pumps

Ass. Prof. Dr. Ali Abdul Mohsin Hassan
Department of Mechanical Engineering
College of Engineering \ Baghdad University
dralicit@yahoo.com

Nabeel Ahmed Kamal
Department of Mechanical Engineering
College of Engineering \ Baghdad University
nabeelahmed1976@yahoo.com

ABSTRACT

Experimental and numerical investigations of the centrifugal pump performance at non-cavitating and cavitating flow conditions were carried out in the present study. Experiments were performed by applying a vacuum to a closed-loop system to investigate the effects of the net positive suction head available (NPSHa), flow rate, water temperature and pump speed on the centrifugal pump performance. Accordingly, many of the important parameters concerning cavitation phenomenon were calculated. Also, the noise which is accompanied by cavitation was measured. Numerical analysis was implemented for two phase flow (the water and its vapor) using a 2-D simulation by ANSYS FLUENT software to investigate the internal flow of centrifugal pump under cavitating conditions. It was observed that with decreasing NPSHa, the values of the pump head, flow rate and efficiency initially remain constant, but with further reduction in NPSHa these parameters will decrease. Also, it was found that at 3% head drop the percentage drop of the flow rate is less than 2% whereas the percentage drop of the efficiency is greater than 3%. Numerically, it was noticed that the cavitation regions appear at the leading edge of suction side of the impeller blades which represents the lowest pressure area inside the computational domain of the centrifugal pump.

Key words: centrifugal pump, cavitation, NPSH, FLUENT, experiments

دراسـة عملية و عددية حـول تـأثير ظاهرة التكهف فـي المضخات النابذة

أ.م.د. علي عبد المحسن حسن
قسم الهندسة الميكانيكية / كلية الهندسة / جامعة بغداد

نبيل أحمد كمال
قسم الهندسة الميكانيكية / كلية الهندسة / جامعة بغداد

الخُلاصة

يتناول هذا البحث دراسة عملية وعددية لإداء مضخة نابذة عند ظروف الجريان غير المتكهف والمتكهف. التجارب العملية أجريت بطريقة تقليل الضغط الداخل الى المضخة بواسطة منظومة تفريغ الهواء، حيث تم دراسة تأثير تغيير قيم رفع السحب الصافي الموجب المتوفر (NPSHa) و معدل الجريان الحجمي و درجة حرارة الماء وسرعة المضخة على اداء المضخة النابذة وعليه عدة متغيرات مهمة تخص ظاهرة التكهف تم أحتسابها، وكذلك تم قياس مستوى الضوضاء المصاحبة لظاهرة التكهف. التحليل العددي لهذه الدراسة تضمن إجراء محاكاة ثنائية الأبعاد للجريان ثنائي الطور (للماء وبخاره) باستخدام حقيبة (ANSYS FLUENT) لتحري ظروف الجريان المتكهف داخل المضخة النابذة. النتائج العملية أظهرت أنه عند تقليل قيمة (NPSHa) فإن قيم رفع المضخة ومعدل الجريان والكفاءة تبقى ثابتة بشكل أولي، ولكن مع أستمرار تقليل قيمة (NPSHa) فإن هذه القيم سوف تنخفض. كذلك لوحظ أنه عند هبوط رفع المضخة بنسبة 3% فأن نسبة هبوط معدل الجريان تكون أقل من 2% في حين أن نسبة هبوط الكفاءة تكون أكثر من 3%. المحاكاة العددية أظهرت أن مناطق التكهف تظهر عند الحافات الأمامية لريش البشارة من جهة السحب حيث أنها تتشكل في المساحة الأقل ضغطا داخل المضخة.

الكلمات الرئيسية: مضخة نابذة، تكهف، رفع السحب الصافي الموجب المتوفر، فلونت، تجارب

1. INTRODUCTION

In many engineering applications, cavitation represents the subject of extensive experimental and numerical researches because it is one of the most serious problems encountered in the operation of pumps. Cavitation refers to the formation of vapor bubbles in regions within the flow field of a liquid, when the liquid absolute pressure drops to reach the vapor pressure corresponding to the operating temperature of this liquid. In some respects, it is similar to boiling except that the latter is generally considered to occur as a result of an increase of temperature rather than a decrease of pressure, **Brennen, 1994**. Cavitation occurs in any situation where fluid is moving relatively to a solid surface (particularly impeller and casing). As the vapor bubbles are transported through the impeller, they reach a zone of higher pressure where they collapse abruptly. If the collapse occurs on the surface of a solid, the liquid rushing in to fill the vacuous space left by the bubbles impacts tiny areas with tremendous localized pressures and thereby pits and erodes the surface. Cavitation reduces pump head, capacity and efficiency because a large number of vapor bubbles will block the impeller channels, which leads to a sudden drop in the pump performance at the cavitation critical point. In addition to the pitting and erosion, cavitation can also cause noise and vibration, **Sanks, et al. 1998.** Cavitating flows in centrifugal pumps were studied by experimental and numerical methods. **Guelich, in 1989** introduced an experimental study dealt with the erosion rate in an impeller of a centrifugal pump based on cavity length and he correlated damaged impellers by deducing the cavity length ,**Sloteman 2007,and . Harihara, and Parlos, 2006,** presented an experimental study of the sensor less approach to detect variable levels of cavitation in centrifugal pumps. The onset of pump cavitation was detected using only the line voltages and phase currents of the electric motor driving the pump. **Cernetic, et al., 2008** introduced experimentally the detection and monitoring of cavitation in centrifugal pumps by using noise and vibration signals. It was found that the noise and vibration levels increase with decreasing NPSHa value. **Houlin, et al., 2010,** presented a numerical simulation and experimental verification dealt with the effects of blade number on characteristics of a centrifugal pump in non-cavitation and cavitation conditions. It was noticed that with the increase of blade number, the area of low pressure region grows continuously, where the clog phenomenon becomes obvious in flow passage of impeller with the more blade number.

2. EXPERIMENTAL WORK

An experimental work was carried out to investigate and study the cavitation phenomenon and its effect on the centrifugal pump performance at different operation conditions. The experimental rig was designed and installed in this work, which allows to carry out the experiments by applying a vacuum to a closed-loop system where this method is usually used to attain cavitation phenomenon in the pumps. **Fig. 1** shows schematically the experimental rig, and this rig is shown photographically in **Fig. 2**. The test pump is a horizontal single-stage volute casing centrifugal pump with an open radial impeller which has three blades. As shown in **Fig.1**, the test pump is connected to the cylindrical vacuum tank which in turn is connected to the single stage dry vacuum pump which used to achieve the required vacuum inside the system. An electrical heater (with thermostat) was attached to the tank to change the temperature of water (the working fluid) for different operation conditions. A transparent Perspex pipe was installed in the suction pipe to observe the water that coming from the vacuum tank to assure that there are no bubbles present in the flow. In order to change the speed of the centrifugal pump, a motor speed controller was attached to the test rig to vary the pump speed to the desired value. The flow rate was adjusted by using the discharge gate valve.

Numerous measuring devices were used in this work, which are as follows: flow meter (rotameter) to measure the water flow rate, pressure gauges to measure the pump suction and discharge pressures and also the vacuum tank pressure, thermometer to measure the water temperature, digital photo tachometer to measure the pump speed, digital sound level meter (decibel meter) to measure the

pump noise and digital clamp meter to measure the voltage and current of the pump motor.

Different experiments were carried out on the experimental rig which involve changing the flow rate with values (10.95, 11.95, 12.95, 13.95 and 14.95 m^3/h), water temperature with values (25.5, 35.5 and 45.5 ˚C) and pump speed with values (2560 and 2660 rpm), as well as the effect of decreasing NPSHa with range (10 to 1 m) which occurs as a result of vacuum process to investigate the effect of these parameters on the centrifugal pump performance at non-cavitating and cavitating flow conditions. Cavitation condition was adjusted by decreasing NPSHa (i.e., pump suction pressure) at the pump suction port as a result of vacuum process.

After accomplishing all of the experiments and the experimental readings were recorded, the calculations were performed to predict the centrifugal pump performance and the equations that used to analyze the experimental readings and to calculate the parameters are illustrated below:

The total pump head (H) of the centrifugal pump is calculated as follows **Kubota, 1972**:

$$H = \frac{P_d - P_s}{\rho g} + \text{Height difference between}$$

$$\text{measuring points} \qquad (1)$$

The net positive suction head available (NPSHa) can be computed by the following equation (White 1998):

$$NPSHa = \frac{P_s}{\rho g} + \frac{v_s^2}{2g} - \frac{P_V}{\rho g} \qquad (2)$$

There are two important parameters are usually used in the cavitating flow field, which are Thoma cavitation number (σ_{TH}) and cavitation number (σ), and these two dimensionless numbers are defined as follows, **Schiavello and Visser, 2008:**

$$\sigma_{TH} = \frac{NPSHa}{H} \qquad (3)$$

$$\sigma = \frac{P_s - P_V}{\frac{1}{2}\rho U^2} \qquad (4)$$

where U is the inlet-blade tip speed = ΩR_{1T} , and R_{1T} represents the inlet-blade tip radius.

Another parameter called suction specific speed (N_{SS}) which is a dimensionless quantity that describes the suction characteristics of a pumping system. This parameter can be computed by the following equation, **Schiavello and Visser, 2008:**

$$N_{SS} = \frac{\Omega Q^{\frac{1}{2}}}{(g\ NPSHa)^{\frac{3}{4}}} \qquad (5)$$

The pump efficiency (η_p) which represents the hydraulic efficiency is calculated as follows, **Girdha and Moniz, 2005:**

$$\eta_P = \frac{P_H}{P_M} = \frac{\rho g Q H}{VI\cos\theta\,\eta_e} \qquad (6)$$

Where, P_H is the pump hydraulic power (water horsepower) and P_M is the motor power (brake horsepower).

Because the inlet and outlet boundaries of the computational domain in the numerical simulation were considered to be at the suction and discharge ports of the centrifugal pump and for comparison between the experimental and numerical results, the pressure measuring points in the experimental work also were considered to be at these boundaries, where the head loss due to friction in the suction and discharge pipes between pressure gauges and the suction and discharge ports of the pump was taken in consideration.

Among the mentioned parameters, the most common parameters that are widely utilized to describe the cavitation progress stages are NPSHa, (σ_{TH}) and (σ). Therefore, in the present study the values of NPSHa and (σ_{TH}) were utilized for comparison with the other parameters, where some parameters were plotted versus the NPSHa and the remaining were plotted versus the (σ_{TH}) especially with the dimensionless parameters. It is important

to note that all curves were plotted to terminate at the critical point that corresponding to the 3% drop in pump head (i.e., at NPSHr value), where this point can be determined experimentally by reducing the pump suction pressure below the critical pressure and then determining the critical point for each curve after calculating the value of 3% head drop.

3. NUMERICAL SIMULATION

The numerical work of the present study aims to analyze the cavitating behavior inside the centrifugal pump by using a numerical simulation which represents an important tool to disclose the mechanism of cavitation characteristic in pumps. To do this, ANSYS FLUENT software release 13.0 was used to simulate the two phase flow (the water and its vapor) inside the centrifugal pump. The cavitation model implemented in FLUENT is based on the so-called "full cavitation model" which developed by **Singhal, et al. in 2001** ,**Stuparu, et al. 2011** and it accounts for all first-order effects like phase change, bubble dynamics, turbulent pressure fluctuations and non-condensable gases. Cavitation was modeled in this work with the help of homogeneous mixture multiphase model. The standard (k-ε) turbulence model and SIMPLEC algorithm were chosen in FLUENT.

In the present work, a 2-D model of the centrifugal pump including a spiral volute casing and curved blades impeller was implemented. The geometry of the pump was created by using professional software "SolidWorks", version 2011. The meshes required for the calculations were generated by using the CFD pre-processing package, "GAMBIT", version 2.4.6. An unstructured 2-D triangular-pave mesh was used for the generation on the computational domain surface as well as a boundary layer mesh was created around the blades. The created computational domain of the centrifugal pump has three zones: inlet zone (pump inlet port), blades zone (pump impeller) and outlet zone (volute casing and pump outlet port), and the total number of nodes in the domain are 24927. The geometrical parameters of the used impeller are shown in **Table 1**.

Table 1. Geometrical parameters for the used impeller**.**

Parameter	Value
Blade shape	Circular arc (non-twisted)
Impeller inlet diameter (mm)	46
Impeller outlet diameter (mm)	120
Blade thickness (mm)	3
Blade inlet width (mm)	11.5
Blade outlet width (mm)	11.5
Number of blades	3

In this work, the study by FLUENT was implemented with two boundary conditions. The first boundary condition is (pressure inlet-pressure outlet) which was employed to plot many contours to illustrate the cavitation regions inside the computational domain under different conditions. The second boundary condition is (velocity inlet-pressure outlet) which was employed to make FLUENT software predicts the inlet pressure of the pump and hence important parameters can be predicted numerically. Both boundary conditions are based on the experimental results.

4. RESULTS AND DISCUSSION

4.1 Experimental Results

Fig. 3 indicates the influence of NPSHa on the pump head for different flow rates, which shows that when the NPSHa decreases, the head values initially remain approximately constant (no cavitation is present at this stage). A further reduction in the NPSHa will decrease the head, where this process continues until the 3% drop in head has been reached. Reducing NPSHa means that decreasing the inlet pressure (suction pressure) of the pump according to **Eq.2,** and this will result in creating and growing the regions of vapor bubbles inside the pump. A large number of vapor bubbles will block the impeller channels, which leads to a sudden drop in the pump head. This figure also illustrates that when the flow rate increases, the NPSHa decreases because the pump inlet pressure will decrease with increasing the flow

rate (due to increasing the velocity of flow). Although the pump inlet velocity increases with increasing the flow rate, but this increasing in inlet velocity will be smaller than the decrease that occurs in the inlet pressure, so NPSHa will decrease as the flow rate increases according to **Eq.(2)**. In addition, it is found that the value of NPSHr (which indicated by black dot) increases with increasing the flow rate where the inlet critical pressure increases with increasing the flow rate. Accordingly, it is concluded that NPSHa is inversely proportional to flow rate, whereas NPSHr is directly proportional to flow rate. According to the numerical results, the inception of cavitation occurs at NPSHa (which called NPSHi) is approximately equal to (3.22 m) for flow rate (12.95 m^3/h), where the flow with NPSHa less than (3.22 m) represents a cavitating flow for all flow rates as indicated in this figure.

Fig. 4 indicates the influence of NPSHa on the pump head for different temperatures, which illustrates that the values of both NPSHa and NPSHr decrease with increasing the temperature because the vapor pressure will increase with increasing the temperature, where vapor pressure is a direct function of temperature. This figure also shows that there are no significant changes in the head values with increasing the temperature at the studied values.

Fig. 5 indicates the influence of NPSHa on the pump head for different pump speeds, which shows that decreasing the speed leads to increase the NPSHa and decrease the NPSHr; where the decrease in speed leads to increase the pump inlet pressure and decrease the inlet critical pressure. Also, it is seen that decreasing the speed leads to decrease the head because the pump outlet pressure (discharge pressure) will decrease with decreasing the speed, where the decrease in outlet pressure will be greater than the increase in inlet pressure which occurs as a result of decreasing the speed.

Fig.6 indicates the influence of NPSHa on the pump flow rate for different flow rates, which illustrates that the flow rate curves have the same behavior of the head curves concerning the effect of decreasing NPSHa which leads to a sudden drop in

the pump flow rate due to blocking the impeller channels with vapor bubbles.

Through comparative study of **Figs.3** and **6** concerning the influence of decreasing NPSHa on the head and flow rate curves, it has been attributed to the fact that when the 3% drop in head has been achieved, the percentage of flow rate drop is less than 2% at the same critical point. As an example, in **Fig.7** which shows the influence of decreasing NPSHa on the head and flow rate curves for the case of flow rate (12.95 m^3/h), this figure clearly shows that the percentage of drop for flow rate is less than that in the head which is equal to 1.16% for this case. This can be explained that the pump head has higher sensitivity to cavitation than flow rate.

Fig. 8 indicates the influence of NPSHa on the pump efficiency for different flow rates, which shows that the efficiency curves have the same behavior of the head and flow rate curves concerning the effect of decreasing NPSHa, where the percentage of efficiency drop at 3% head drop is more than 3% because the drop in both the head and flow rate has been considered in calculating the efficiency according to **Eq. (6).** As an example, the percentage of efficiency drop for the curve with flow rate (12.95 m^3/h) is equal to 4.08%. This figure also shows that the curves with flow rates (11.95 and 12.95 m^3/h) have the highest efficiency values, and the curves with flow rates (10.95 and 13.95 m^3/h) come below them, while the curve with flow rate (14.95 m^3/h) has the lowest efficiency value. The reason for this is that the two highest efficiency curves have flow rates that are too close to the best efficiency point (BEP) flow rate; whereas the other three curves have flow rates relatively far from the BEP flow rate. It is quite apparent that the BEP flow rate is located between the flow rates (11.95 and 12.95 m^3/h).

Fig.9 indicates the influence of NPSHa on the Thoma cavitation number for different flow rates, which illustrates that the Thoma cavitation number decreases linearly as NPSHa decreases because it is directly proportional to NPSHa according to

Eq.(3). Also, it is shown that when the flow rate increases the Thoma cavitation number increases too because the increase in flow rate causes a reduction in the head which leads to increase Thoma cavitation number. Although the increase in flow rate will result in decreasing the NPSHa as discussed previously, but the decrease in head will be greater than that in NPSHa as a result of increasing the flow rate. Also, this figure illustrates that the critical point of the Thoma cavitation number (at 3% head drop) increases with increasing the flow rate because this critical point has been calculated according to NPSHr which is directly proportional to flow rate.

Fig. 10 indicates the influence of NPSHa on the pump noise level for different flow rates, which shows that when the NPSHa decreases the noise level increases, where the noise level starts to increase rapidly at NPSHa is approximately (9 m), and this behavior continues with decreasing NPSHa until it reaches approximately (6 m), then noise level increases slowly until NPSHa reaches approximately (3 m), after that the noise level starts again to increase rapidly with decreasing NPSHa due to a large number of vapor bubbles will collapse as they enter the region of higher pressure. This figure also shows that the difference in the pump noise level between non-cavitating and cavitating flow (at 3% head drop) is about 8 dB. Also, it is seen in this figure that the noise level decreases slightly with increasing the flow rate.

Fig.11 indicates the influence of Thoma cavitation number on the cavitation number for different flow rates, which illustrates that the cavitation number decreases linearly as Thoma cavitation number decreases that is because cavitation number depends on the pump inlet pressure according to **Eq. (4),** and Thoma cavitation number is directly proportional to NPSHa which in turn depends on the inlet pressure. Also, it is shown that the cavitation number decreases with increasing the flow rate because the pump inlet pressure decreases with increasing the flow rate (due to increasing the velocity of flow). On the other hand, the critical point of the cavitation number (at 3% head drop) has been calculated according to the pump inlet pressure that corresponding to the NPSHr, hence it increases

with increasing the flow rate as shown in this figure because NPSHr is directly proportional to flow rate.

Fig.12 indicates the influence of Thoma cavitation number on the suction specific speed for different flow rates, which shows that the suction specific speed increases nonlinearly as Thoma cavitation number decreases. Decreasing Thoma cavitation number means that decreasing NPSHa as discussed previously, and according to **Eq.(5)** the suction specific speed is inversely proportional to NPSHa, hence decreasing any of these two parameters (Thoma cavitation number or NPSHa) leads to increase the suction specific speed. Also, it is shown that the suction specific speed increases with increasing the flow rate because it is directly proportional to flow rate. On the other hand, the critical point of the suction specific speed (at 3% head drop) has been calculated according to NPSHr, hence this critical point decreases with increasing the flow rate, where the effect of NPSHr will be slightly greater than the flow rate in **Eq.(5).**

4.2 Numerical Results and Comparison

Figs. 13 to **15** indicate the influence of decreasing NPSHa on the inception and growth of cavitation regions (vapor regions) inside the computational domain of the centrifugal pump according to the first boundary condition. **Figs. 13**, **14** and **15** illustrate the computational domain at NPSHa values (3.22 m), (2.27 m) and (1.45 m) respectively. In these figures, it is shown that the cavitation regions appear at the leading edge of suction side of the impeller blades which represents the lowest pressure area inside the domain and the area of these regions expands as a result of decreasing NPSHa, where the value of NPSHa (1.45 m) is equal to NPSHr according to the experimental results of this test. On the other hand, it was found that these cavitation regions expand with increasing the temperature whereas they reduce with decreasing the speed because the NPSHa decreases with increasing the temperature and it increases with decreasing the speed as it is concluded in the experimental results.

Fig. 16 indicates the influence of decreasing NPSHa on the head numerically according to the second boundary condition. In this figure, it is

shown that the head remains approximately constant with decreasing NPSHa, but with further reduction in the NPSHa the head will decrease, where this process continues until the 3% drop in head has been reached. After the critical point, the drop in the head will be more rapidly with decreasing NPSHa.

Fig. 17 shows the comparison between the experimental and numerical result of the (Head-NPSHa) curve, which illustrates that the numerical head curve follows the same behavior of the experimental head curve but with some differences between them, where the numerical curve falls below the experimental curve with an average difference of (9%), and its critical point exceeds the critical point of the experimental curve with a difference of (16.6%). The difference between the numerical and experimental result in this figure is may be due to simplifying the solution of this simulation from three-dimensional to two-dimensional approach.

5. CONCLUSIONS

The main study conclusions can be summarized as follows:

(1) With decreasing NPSHa, the pump head, flow rate and efficiency will decrease where it was found that at 3% head drop, the percentage drop of flow rate is less than 2% whereas the percentage drop of efficiency is greater than 3%.

(2) NPSHa decreases with increasing the flow rate and temperature and it increases with decreasing the speed, whereas NPSHr increases with increasing the flow rate and it decreases with increasing the temperature and decreasing the speed.

(3) Pump noise level increases with decreasing NPSHa and flow rate.

(4) Cavitation regions appear at the leading edge of suction side of the impeller blades which represents the lowest pressure area inside the computational domain of the centrifugal pump, where these cavitation regions expand with decreasing the NPSHa and increasing the temperature whereas they reduce with decreasing the speed.
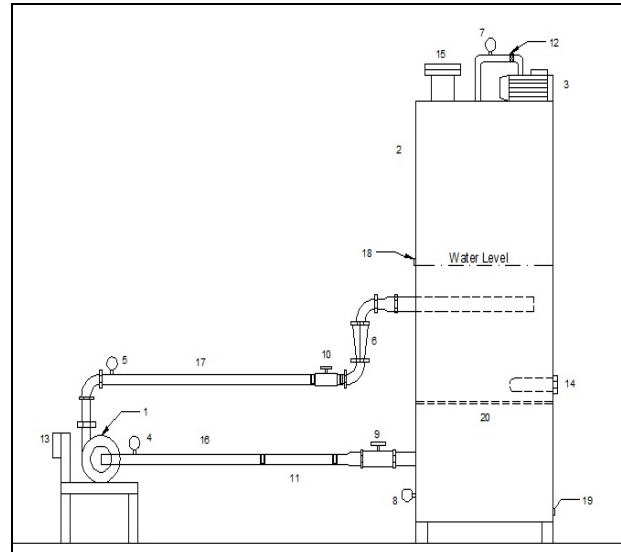
1	Centrifugal Pump (Test Pump)	11	Transparent Perspex Pipe
2	Vacuum Tank	12	Pneumatic Valve (0.5 in)
3	Vacuum Pump	13	Motor Speed Controller
4	Suction Pressure Gauge	14	Electrical Heater & Thermostat
5	Discharge Pressure Gauge	15	Filling & Ventilation Opening (4 in)
6	Flow Meter (Rotameter)	16	Suction Pipe (1.5 in)
7	Tank Pressure Gauge	17	Discharge Pipe (1.5 in)
8	Thermometer	18	Water Level Indicating Hole
9	Suction Gate Valve (2 in)	19	Drain Hole
10	Discharge Gate Valve (1.5 in)	20	Stainless Steel Strainer

Figure 1. Schematic representation of the experimental rig.

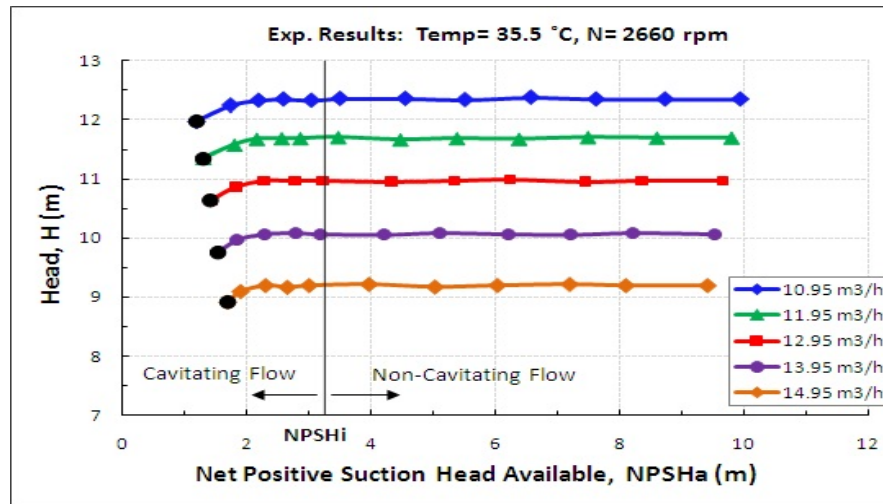**Figure 2**. Photograph of the experimental rig.

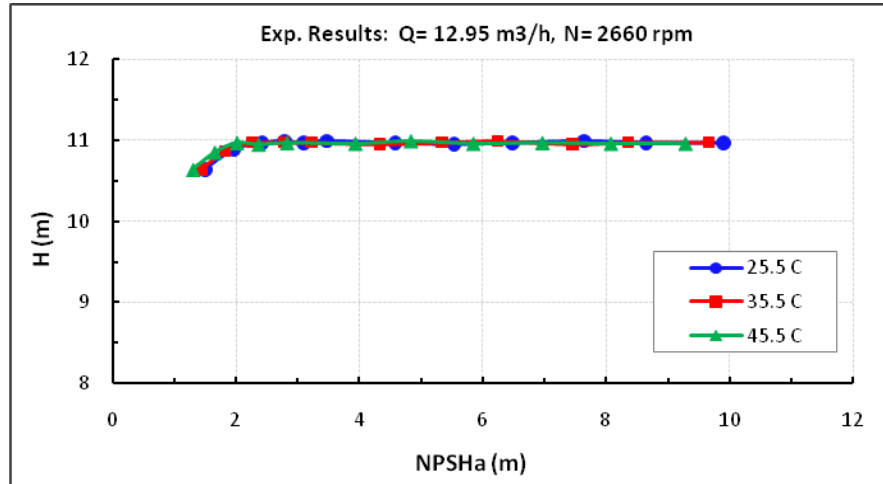**Figure 3.** Influence of NPSHa on the head for different flow rates.

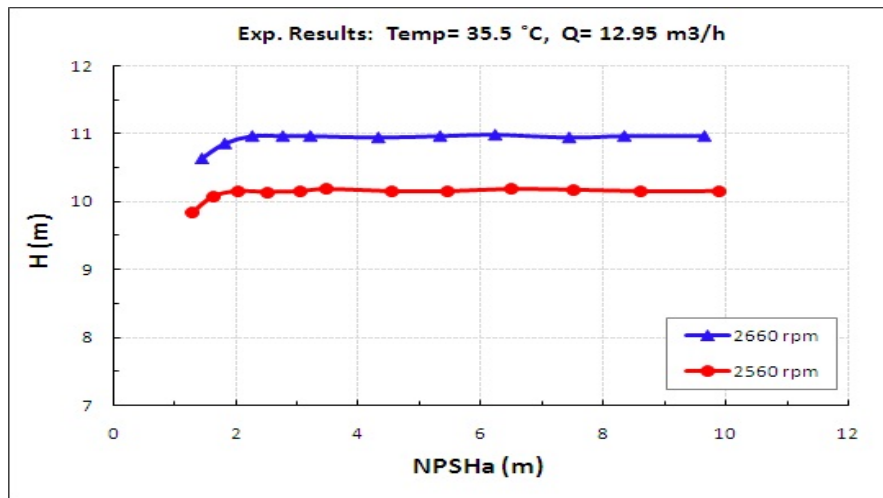**Figure 4.** Influence of NPSHa on the head for different temperatures.

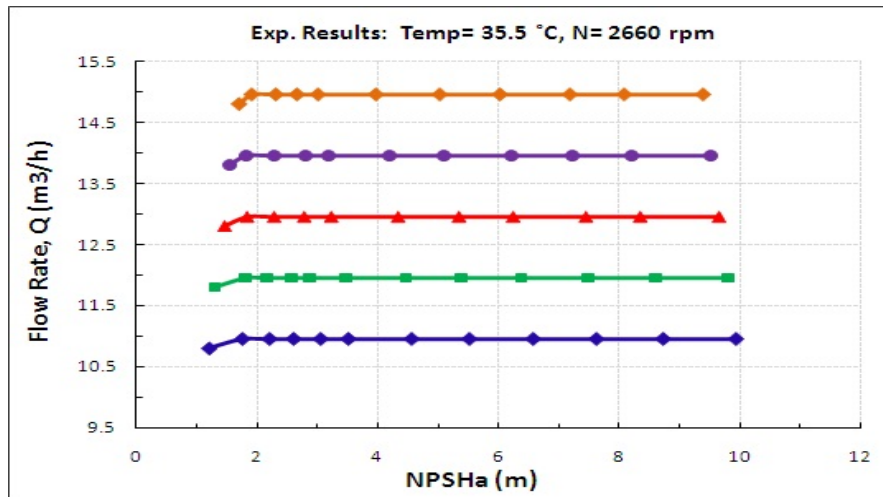**Figure 5**. Influence of NPSHa on the head for different speeds.

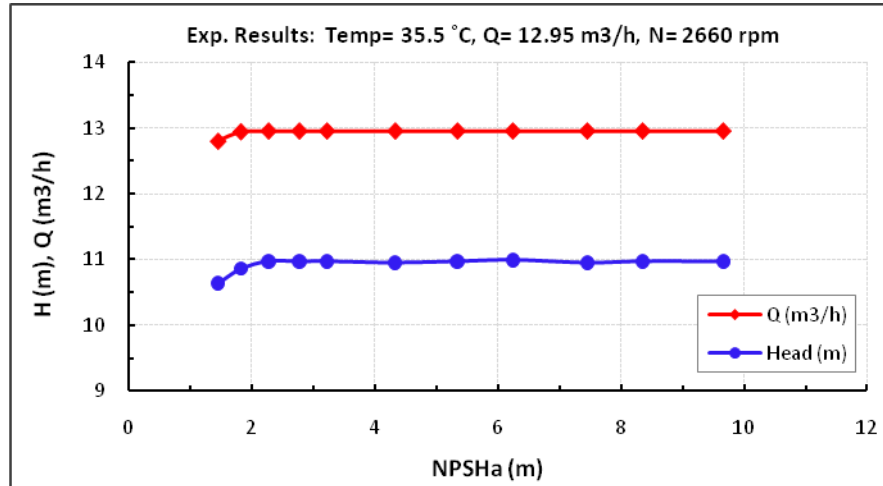**Figure 6.** Influence of NPSHa on the flow rate for different flow rates.

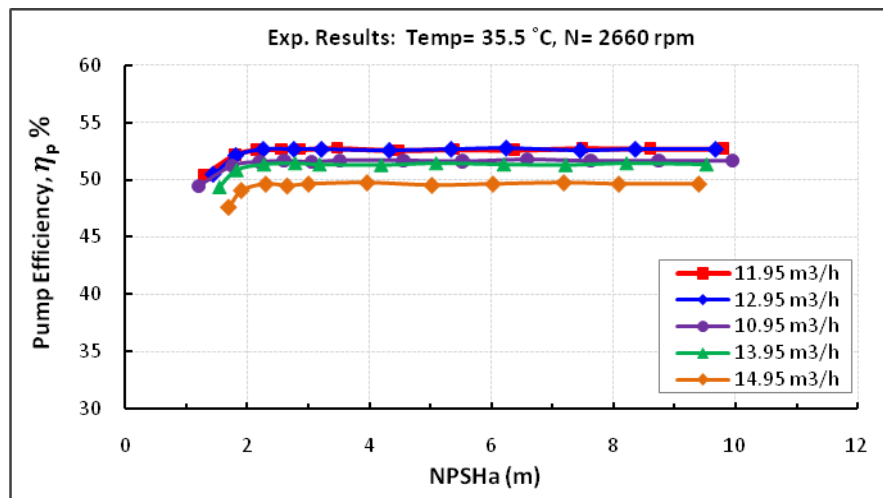**Figure 7.** Influence of NPSHa on the head and flow rate.

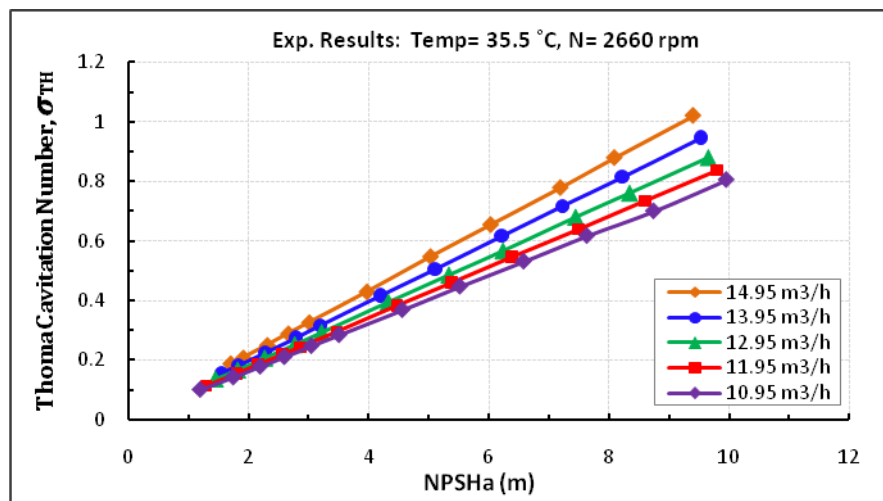**Figure 8.** Influence of NPSHa on the efficiency for different flow rates.

Figure 9. Influence of NPSHa on the Thoma cavitation number for different flow rates.

82
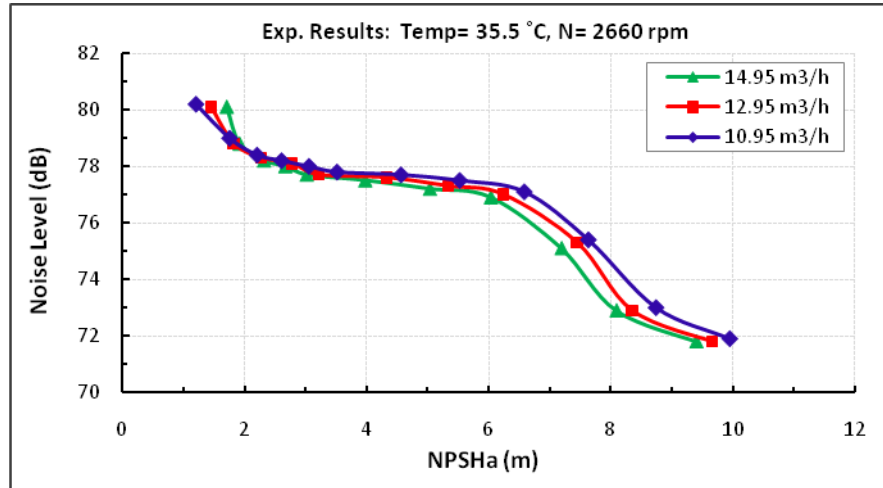
Figure 10. Influence of NPSHa on the pump noise level for different flow rates.
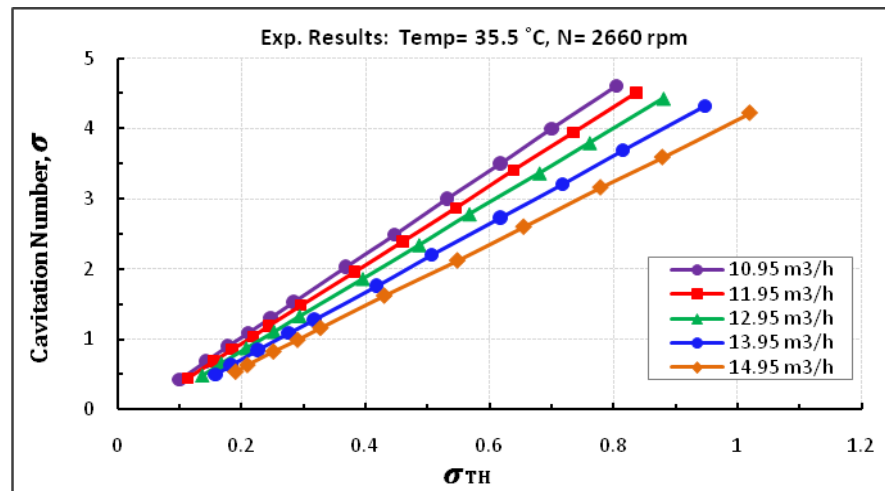
Figure 11. Influence of Thoma cavitation number on the cavitation number for different flow rates.
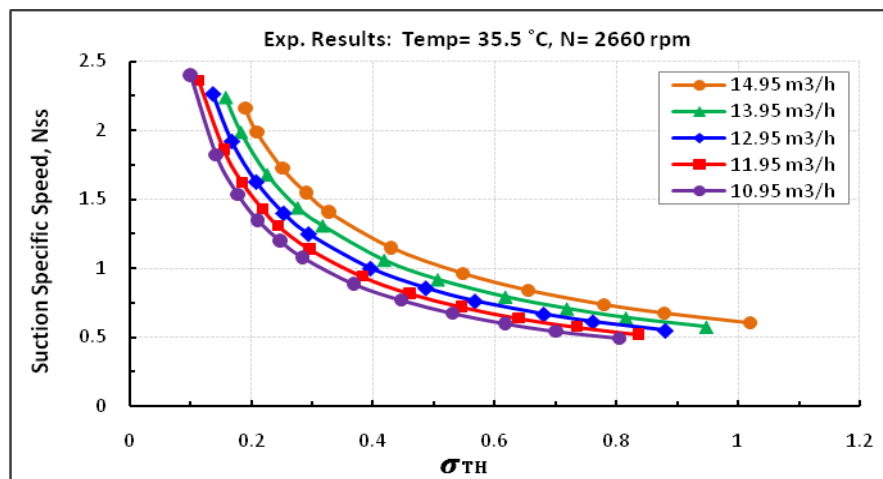
Figure 12. Influence of Thoma cavitation number on the suction specific speed for different flow rates.
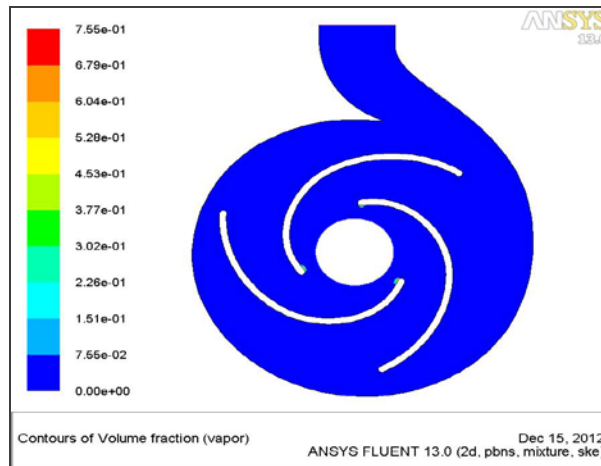
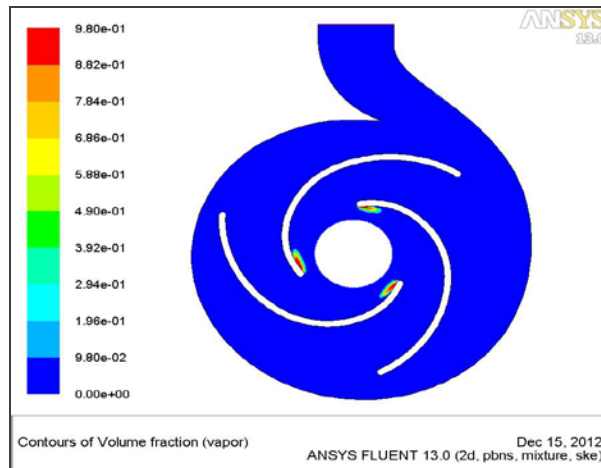**Figure 13.** Cavitation regions (NPSHa = 3.22 m, 35.5 ˚C and 2660 rpm).

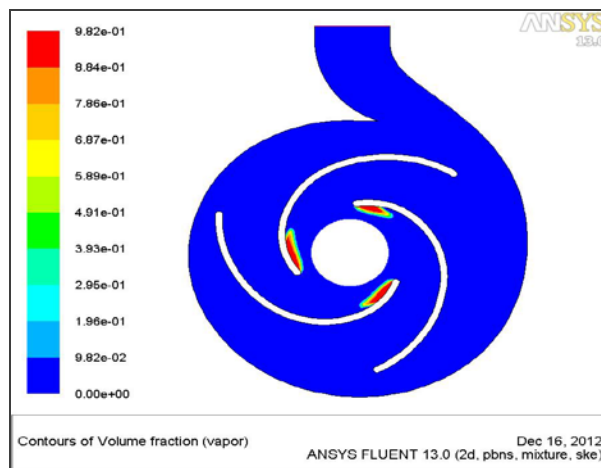**Figure 14.** Cavitation regions (NPSHa = 2.27 m, 35.5 ˚C and 2660 rpm).

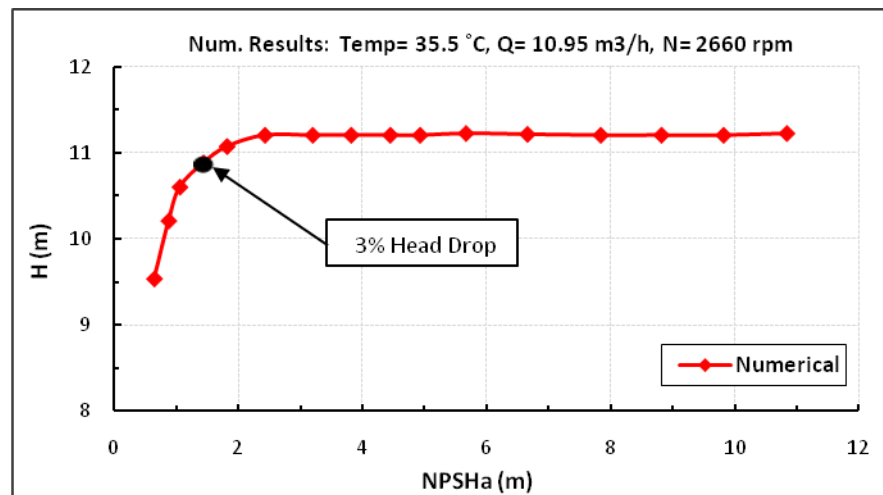**Figure 15**. Cavitation regions (NPSHa = 1.45 m, 35.5 ˚C and 2660 rpm).

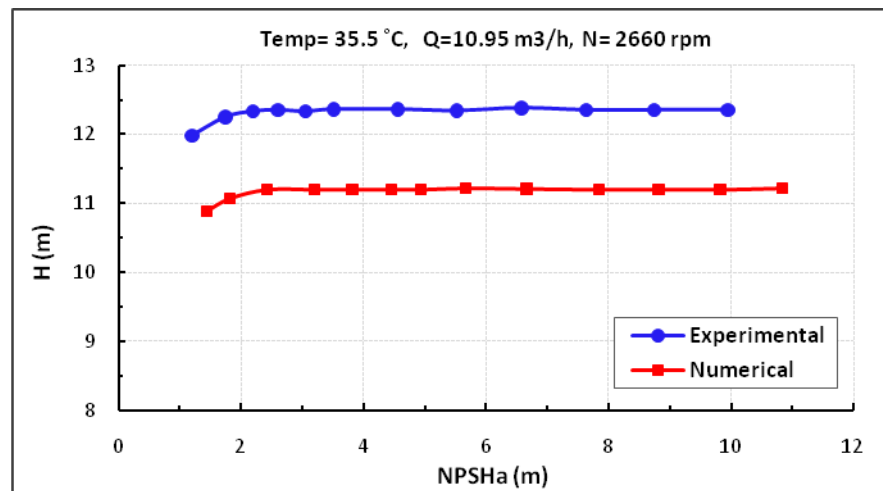**Figure 16.** Influence of NPSHa on the head.

Figure 17. Comparison between experimental and numerical (Head-NPSHa) curve.

REFERENCES

Brennen, C.E., 1994, "*Hydrodynamics of Pumps*", Concepts NREC and Oxford University Press.

Cernetic, J., Prezelj, J., and Cudina, M., 2008, "*Use of Noise and Vibration Signal for Detection and Monitoring of Cavitation in Kinetic Pumps*", University of Ljubljana, Faculty of Mechanical Engineering, Slovenia, pp. 2199-2204, June 29-July 4.

Girdhar, P., and Moniz, O., 2005, First Edition, "*Practical Centrifugal Pumps*", IDC Technologies, Netherlands.

Harihara, P.P., and Parlos, A.G., 2006, "*Sensorless Detection of Cavitation in Centrifugal Pumps*", ASME International Mechanical Engineering Congress and Exposition, November 5-10, Chicago, USA.

Houlin, L., Yong, W., Shouqi, Y., Minggao, T., and Kai, W., 2010, "*Effects of Blade Number on Characteristics of Centrifugal Pumps*", Chinese Journal of Mechanical Engineering, Vol. 23, pp. 1-6.

"*Kubota Pump Hand Book*", 1972, First Edition, Volume 1, Kubota Ltd. Pump Export Department.

Sanks, R.L., Tchobanoglous, G., Bosserman, B.E., and Jones, G.M., 1998, Second Edition, "*Pumping Station Design",* Butterworth-Heinemann, USA.

Schiavello, B., and Visser, F.C., 2008, "*Pump Cavitation-Various NPSHR Criteria, NPSHA Margins and Impeller Life Expectancy*", Twenty Fourth International Pump Users Symposium.

Sloteman, D.P., 2007, "*Cavitation in High Energy Pumps-Detection and Assessment of Damage Potential*", Twenty-Third International Pump Users Symposium, pp. 29-38.

Stuparu, A., Susan-Resiga, R., Anton, L.E., and Muntean, S., 2011, "*A New Approach in Numerical Assessment of the Cavitation Behavior of Centrifugal Pumps",* International Journal of Fluid Machinery and Systems, Vol. 4, No.1, pp. 104-113, January-March.

White, F.M., 1998, Fourth Edition, "Fluid Mechanics", McGraw-Hill Series.

NOMENCLATURES

g = Acceleration due to gravity (m/s^2)
H = Pump head (m)
I = Current (amp)
k = Turbulent kinetic energy (J/kg)
N = Rotational speed (rpm)
$NPSHa$ = Net positive suction head available (m)
$NPSHi$ = Incipient net positive suction head (m)
$NPSHr$ = Net positive suction head required (m)
N_{SS} = Suction specific speed
P = Static pressure (Pa)
P_H = Pump hydraulic power (watt)
P_M = Motor power (watt)
Q = Volumetric flow rate (m^3/s)
R_{IT} = Inlet-blade tip radius (m)
$Temp$ = Temperature (˚C)
U = Inlet-blade tip speed (m/s)
V = Voltage (volts)
v = Average velocity of flow (m/s)

Greek Symbols

ε = Turbulent dissipation rate (J/kg)
η_e = Motor efficiency
η_p = Pump efficiency

$\cos\theta$ = Power factor
ρ = Density (kg/m^3)
σ = Cavitation number
σ_{TH} = Thoma cavitation number
Ω = Angular speed = $\pi N/30$ (rad/s)

Subscript Symbols

d = Discharge
s = Suction
V = Vapor

Abbreviations

BEP = Best Efficiency Point
CFD = Computational Fluid Dynamics